

## Epoxy Resin with Amphiphilic Ionic Liquid as Hydrophobic Organic Coating for Steel

Ayman M. Atta<sup>1,\*</sup>, Eid M.S. Azzam<sup>2,\*</sup>, Khalaf M. Alenezi<sup>2</sup>, Hani El Moll<sup>2</sup> and A. Haque<sup>2</sup>

<sup>1</sup> Chemistry department, college of science, king Saud university, Riyadh11545, Saudi Arabia.

<sup>2</sup> University of Hail, college of science, department of chemistry, 81451 Hail, Saudi Arabia.

\*E-mail: [aatta@ksu.edu.sa](mailto:aatta@ksu.edu.sa) (A.M.A.) and [eazzamep@yahoo.com](mailto:eazzamep@yahoo.com) (E.M.S.A).

Received: 1 March 2021 / Accepted: 7 April 2021 / Published: 30 April 2021

---

The ionic liquids (ILs) have been proposed as curing modifiers to obtain superior epoxy coatings. In the present work, the imidazolium and pyridinium cations combined in amphiphilic hardener based on polyamines to apply as curing for epoxy resin and to obtain organic coatings on the steel surface. In this respect, the primary amine groups of triethylenetetramine, pentaethylenehexamine or aminopyridinium tetradecylbromide was condensed with p-hydroxybenzaldehyde and glyoxal to obtain new ILs. The phenol group of the produced ILs were etherified with tetraethylene glycol to obtain amphiphilic ILs. The chemical structure, thermal stability, and thermal characteristics as new ILs were characterized. The curing exotherms of the epoxy resins with the liquid ILs were evaluated from diffraction scanning calorimetric (DSC) and thermostated curing system to determine the maximum curing exothermic temperatures and times. The cured epoxy coatings were applied on the steel surfaces to investigate their adhesion strengths, morphologies and seawater salt spray resistance. The data confirm that the cured epoxy resin in the presence of ILs hardeners show higher adhesion strengths and salt spray exposure time more than 15 MPa and 2000h, respectively.

---

**Keywords:** Epoxy; Ionic liquids; Imidazolium and pyridinium cations; Coatings; Adhesion.

### 1. INTRODUCTION

Epoxy coatings have been widely used as primer for coatings of the steel pipelines and equipments of petroleum and petrochemicals process [1-3]. The fast curing of epoxy resins was produced in the presence different types of polyamines hardeners is responsible for occurring surfaces damages such as cracks, holes and tough surfaces [4]. There are different types of inorganic fillers added during the curing of epoxy to improve their mechanical properties [5]. These fillers were used with large quantity and affect the adhesion of epoxy coatings with different substrates [5]. Nanomaterials based on inorganic metal and metal oxides such as zirconia, titania, iron oxides and zinc oxides were used to

improve the mechanical properties of epoxy [6]. The dispersion of nanomaterials and their tendency to agglomerate during the epoxy coatings limit the application of these materials which improved by using capping materials and carbon nanomaterials based on graphene and carbon nanotubes [7-9]. Recently, ionic liquids (ILs) were used to promote the curing of epoxy resins with polyamine and polyamides hardener [10-13]. The ILs are organic salts included imidazolium, pyridinium, phosphonium and quaternary ammonium as cations were applied as catalyst for ring opening of epoxide and they were used as green materials due to their greater thermal stability and low vapour pressure. ILs were used in epoxy coating formulations because they offer low viscosity formulations and exhibited long term stability at room temperature [14]. The main objective of the present work is to modify the thermal, mechanical, anti-corrosion and surface properties of the epoxy coatings by using amphiphilic ILs combined two types of imidazolium and pyridinium cation.

Imidazolium ionic liquids (IILs) were used as catalyst to enhance and promote the rate and reaction yield of the cured epoxy [15-17]. The IILs contain acetate anion were used as curing agent for epoxy resin at higher temperature (150 °C) through dealkylation (removal of methyl or ethyl acetate) to produce dealkylated imidazole that initiate the ring opening of oxirane [18]. Addition of benzaldehyde to IILs based on acetate promote the ring opening polymerization of epoxy resin at room temperature using carbene mechanism [18]. The modification of epoxy resin with IILs was effective route to obtain antimicrobial hydrophobic and thermal stable epoxy coatings [19]. The chemical structures of IILs were modified with phenylphosphate anion to promote the epoxy curing rate as well as to control the epoxy coatings flame retardancy [20]. IILs were also used to exfoliate the montmorillonite clay minerals to improve the mechanical properties of the epoxy coatings [21]. The modification of epoxy coatings with modified IILs containing polyaniline/ carbon nanotube hybrid improve the barrier properties of the epoxy coatings to be more effective anticorrosive coatings for carbon steel in aggressive marine environment [22]. In this respect, the present work aims to prepare new type of ILs combined both imidazolium and pyridinium cations (IPIL) modified with hydrophobic tail based on cetyl group. The head of the IPIL was modified by etherification of its phenol group with polyethylene polyamines to apply as hardener to obtain cured epoxy networks having good adhesion with steel surfaces. The evaluation mechanical, thermal, thermomechanical and anti-corrosive performance of the epoxy coatings on the steel surface is another goal of the present work.

## 2. EXPERIMENTAL

### 2.1. Materials

All chemicals used to prepare the IILs were purchased from Sigma-Aldrich Chemicals Co. Cetyl bromide (CBr) was used to quaternize 4-aminopyridine (4-AP) as described in the previous work [23]. In this respect, 4-AP (20 mmol, 1.88g) was heated with N,N-dimethylformamide (DMF; 50 mL) and CBr (20 mmol, 5.54g) at 100°C for 6 h. The cetyl 4-aminopyridinium bromide (CAP) was precipitated by addition of ethyl ether, and then recrystallized twice from ethanol to obtain a white powder with 85% yield and melting temperature of 138 °C. Glyoxal monohydrate (GO), acetic acid, 4-

hydroxybenzaldehyde (HBA),  $\beta,\beta$ -dichlorodiethylether (DCDE), triethylenetetramine (TETA), pentaethylenhexamine (PEHA) and sodium hydroxide were used to prepare IIL. Seawater was collected from Arabian Gulf at Dammam coast. Commercial Epikote epoxy resin 828 based on diglycidyl ether bisphenol A with epoxy equivalent weight 190–200 g/eq; Hexion, Olana, Italy) was used to prepare epoxy coatings. The carbon steel panels having the following chemical compositions: 0.14% C, 0.57% Mn, 0.21% P, 0.15%, 0.37% Si, 0.06% V, 0.03% Ni, 0.03% Cr and Fe balance were used as coating substrate.

## 2.2. Synthesis of IIL epoxy hardener

The amino group of CAP was condensed with glyoxal and HBA in acetic acid solution followed by amination of the remained phenol group using PEHA or TETA and  $\beta,\beta$ -dichlorodiethylether to obtain amphiphilic dipyrindinium imidazolium IL (AIPy-IL).

### a) Preparation of amphiphilic dipyrindinium imidazolium IL (IPy-IL)

Aldehyde solution was prepared by dissolving glyoxal monohydrate (5 mmol, 0.38g) and p-hydroxybenzaldehyde (0.005 mol; 0.61 g) in 20 mL of aqueous acetic acid and was added to amine solution. CAP (0.01 mol, 3.17g) amine solution in 20 mL of acetic acid aqueous solution and its pH adjusted to 5. The reaction mixture was vigorously stirred and heated at 60 °C for 5 h followed by washing several times with diethyl ether to obtain IPy-IL.

IPy-IL (2 mmol, 1.52g) was mixed with TETA or PEHA (2 mmol), DCDE (2 mmol, 0.286g) and NaOH pellets (4 mmol, 0.16g). The mixture was completely stirred in xylene (20 ml) and refluxed for 6h under vigorous stirring. The reaction mixture was filtrated on hot to separate NaCl and AIPy-IL was obtained by distillation from xylene using rotary evaporator under reduced pressure as brown oil product.

## 2.3. Characterizations the prepared IILs.

The nitrogen content and the total amine number (TAV; mg KOH.g<sup>-1</sup>) of the liquids AIPy-IL based on TETA and PEHA were analysed according to Kjeldahl method according to American Society for Testing and Materials (ASTM D 2074–19) [24]. The TAV was determined according to back titration method of the excess add HCl (0.5 M) that added to known weights of AIPy-IL dissolved in 100 mL of neutral isopropanol in the presence of bromocresol green as an indicator via standard solution of KOH. The chemical structures of IPy-IL and AIPy-IL were confirmed with <sup>1</sup>H and <sup>13</sup>C-NMR (Bruker AVANCE DRX-400) using d<sup>6</sup>-DMSO as a solvent. Thermal stability of IPy-IL and AIPy-IL were determined from thermogravimetric and differential thermogravimetric analysis (TGA-DTG; TGA-50 SHIMADZU) using N<sub>2</sub> at a heating rate of 10 °C.min<sup>-1</sup>, respectively. Thermal characteristics such as glass transition temperature (T<sub>g</sub>) of AIPy-IL was determined by (DSC; Shimadzu DTG-60 M) with the heating rate of 10°C min<sup>-1</sup>.

#### 2.4. Curing and Coatings of DGEb/ AIPy-IL on the steel surfaces

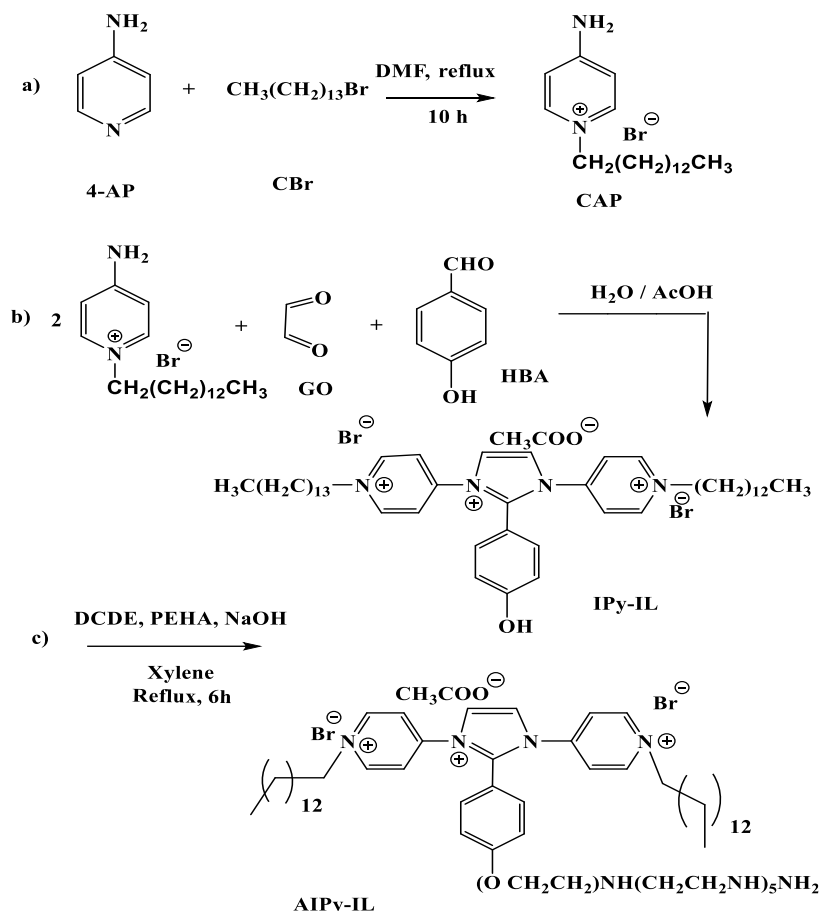
The curing of DGEb with stoichiometric quantity of AIPy-IL was evaluated manually by Digitron digital differential thermometer. The blends of DGEb and AIPy-IL were mixed with magnetic stirrer into isolated glass bottle (5 mL) fitted with a thermometer at different temperatures ranged from 45 to 65 °C. The curing temperature was recorded during the curing time intervals. The temperature of the curing reaction was kept constant and the maximum curing temperature ( $T_{\max}$ ) and time ( $t_{\max}$ ) were determined from their temperature/time curves. The glass bottles volume and the shape used in all experiments were unified to achieve the reproducibility of the measurements. The curing exothermic peaks of DGEb with stoichiometric quantity of AIPy-IL were determined at higher temperature using differential scanning calorimetry (DSC; Q10 DSC calorimeter from TA Instrument, New Castle, DE, USA) based on non-isothermal dynamic mode at a heating rate 5 °C·min<sup>-1</sup> from -30 to 300 °C. The stoichiometric DGEb and AIPy-IL blended manually and low quantity (5–7 mg) was sealed in aluminum cups, sealed, heated under N<sub>2</sub> purge of 50 mL·min<sup>-1</sup>, and the empty cup was used as blank.

The solution of DGEb with stoichiometric quantity of AIPy-IL was sprayed on a clean and rough steel panel (50 μm) to form dry film thickness to 100 μm and kept for 7 days of curing at room temperature. The epoxy coatings on the steel panels were subjected to test their mechanical and anticorrosion performances after complete curing (7 days). Salt spray resistance of the epoxy-coated steel panels was carried out by salt spray cabinet (CW Specialist equipment's Ltd. Model SF/450, Leominster, UK) at 35 °C under humidity 98% of seawater (ASTM B117-03) [25]. The corrosion resistance was evaluated according to the degree of rusting in relation to ASTM D610-95 [26]. The film hardness, impact resistance, the flexibility bend, abrasion resistance, and pull-off adhesion tests were carried out according ASTM D 3363-00 [27], ASTM D2794-04 [28], ASTM D 522-93a [29], ASTM D4060-19 [30], and ASTM D 4541-02 [31], respectively.

### 3. RESULTS AND DISCUSSION

The present work aims to design new amphiphilic ionic liquids combined both imidazolium and pyridinium IL and has hydrophobic and hydrophilic polyamine moieties as represented in Scheme 1. The preparation method for quaternization of 4-AP with long chain alkyl bromide based on CBr was represented in Scheme 1a. The quaternization method reported in the experimental work [23] confirmed that the product of CBr was obtained with yield % (76 %) and its chemical structure indicated that the amino group of 4-AP did not quaternize during the reaction. The amine group of CAP was reacted with aldehyde groups of GO and HBA in the presence of acetic acid solution to produce IPy-IL with yield % of 95 % as represented in scheme 1b. The remained OH phenyl of IPy-IL was aminated with TETA or PEHA in the presence of DCDE as linking agent and NaOH as a catalyst to obtain AIPy-IL (scheme 1c). The products of TETA and PEHA were designated as AIPy-TIL and AIPy-PIL, respectively. The yields of the prepared IPy-IL, AIPy-TIL and AIPy-PIL were summarized and their nitrogen contents (wt. %) were summarized in Table 1. The nitrogen contents determined experimentally agree in harmony with

the calculated values and confirm the purity of the prepared IILs. Moreover, all the prepared IILs are soluble in water as well as organic polar or nonpolar solvents such as ethanol or toluene, respectively.



**Scheme 1.** Synthesis method of IPy-IL and AIPy-IL.

**Table 1.** Physico-chemical characterization of the prepared IILs.

Compounds of IILs	Yield (wt. %)	Nitrogen content (wt. %)		TAV mgKOH/g
		Calc.	Exp.	
IPy-IL	95.0	7.36	7.28	-
AIPy-TIL	85.1	9.88	9.84	1038.8
AIPy-PIL	90.3	11.47	11.56	812.9

### 3.1. Characterization of IILs

The chemical structures of IPy-IL, AIPy-TIL and AIPy-PIL designed in scheme 1 were elucidated from their  $^1\text{H}$ NMR and  $^{13}\text{C}$ NMR spectra represented in **Figures 1 and 2a-b**, respectively. The chemical structure of IPy-IL correlated with its peaks summarized in  $^1\text{H}$ NMR and  $^{13}\text{C}$ NMR spectra

(Figure 1a and b). The acetate anion of IPy-IL was elucidated from the appearance of singlet peak at 2.1 ppm and 21 ppm (Figures 1 and 2). The presence of OH phenol of IPy-IL elucidated also from the appearance of singlet peak at Ph-C-O at 9.8 ppm, and 192 ppm, respectively. The appearance of new peaks in the AIPy-PIL spectrum (Figure 1b) at 4.2, 3.4, 2.75 and 2.7 ppm referred to Ph-OCH<sub>2</sub>, NH<sub>2</sub>, CH<sub>2</sub>CH<sub>2</sub>-N, and NH, respectively confirms the amination of IPy-IL to form AIPy-PIL. Moreover, the peaks at 49.5, 59, 61 ppm referred to C-C-N, C-C-O and C-N<sup>+</sup>, respectively in <sup>13</sup>CNMR spectrum of AIPy-TIL (Figure 2b) also elucidate its amination with TETA and quaternization with CBr.

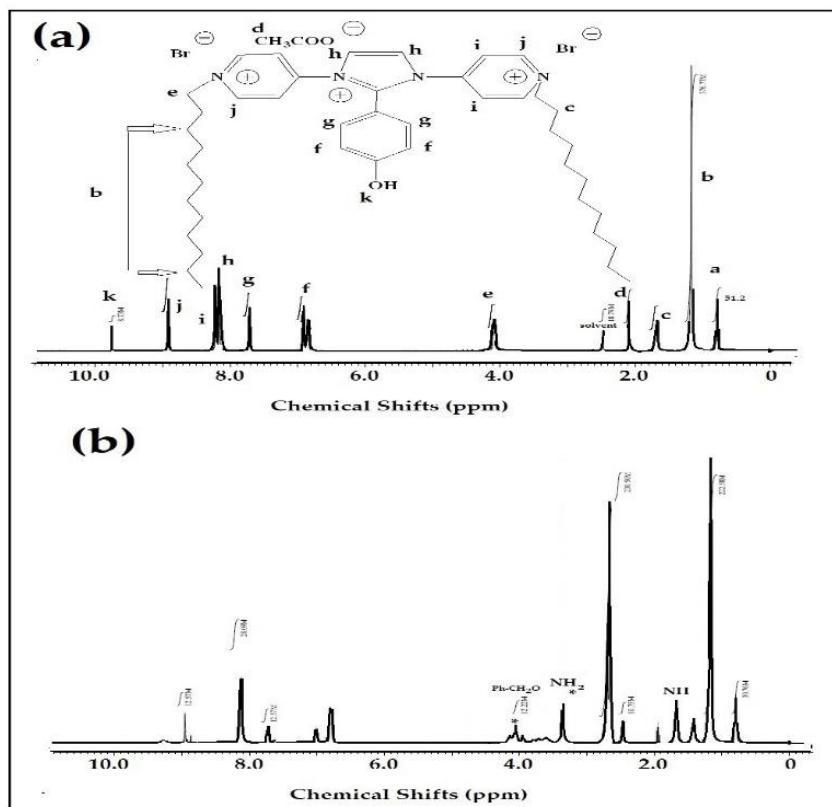


**Figure 1.** <sup>1</sup>HNMR spectra of a) IPy-IL and b) AIPy-PIL

The incorporation of PEHA and TETA in the chemical structure of IPy-IL to obtain AIPy-PIL and AIPy-TIL, respectively and their effect on the thermal characteristics such as glass transition ( $T_g$ ), crystallization ( $T_c$ ) and melting ( $T_m$ ) temperatures were examined from their DSC thermograms summarized in Figure 3a-c. There are three peaks appeared as  $T_g$ , exothermic  $T_c$  and endothermic  $T_m$  peaks at  $-53.9$  °C,  $-13.4$  °C and  $70-71$  °C, respectively in IPy-IL thermograms (Figure 3a) elucidates that IPy-IL behaves as IL. It has low  $T_m$  below  $100$  °C beside the appearance of  $T_g$  below °C. The increasing  $T_g$  values of AIPy-PIL (Figure 3b) and AIPy-TIL (Figure 3c) as appeared at  $-25.2$  and  $-35.6$  °C, respectively than IPy-IL confirms that the amination with PEHA and TETA leads to increase its rigidity. The amination of OH of IPy-IL with PEHA or TETA increases the hydrogen bonding of primary and secondary groups that increased more with AIPy-PIL due to increased length of ethyleneamine [32]. The

$T_c$  of IPy-IL elucidates its higher symmetry, effective charges distribution and strong ion interactions [33].

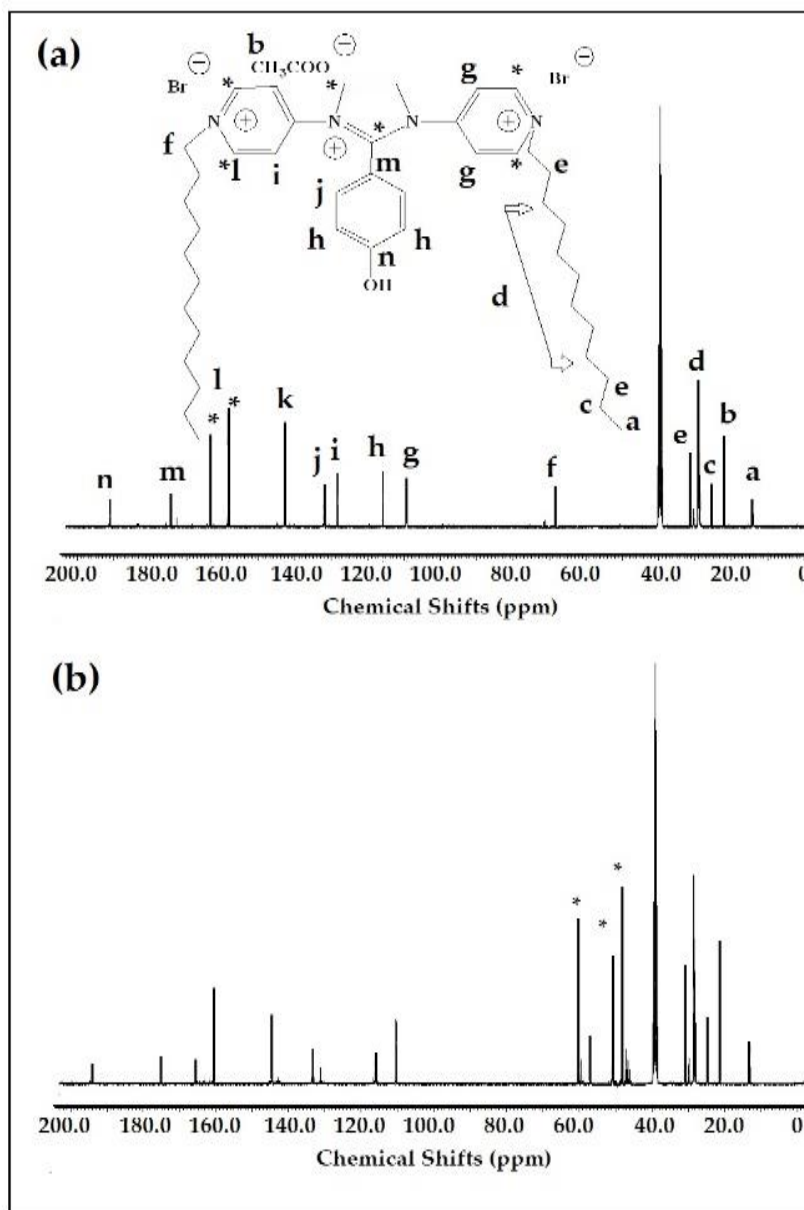


**Figure 2.** <sup>13</sup>CNMR spectra of a) IPy-IL and b) AIPy-TIL.

The thermal stability of was investigated from their TGA-DTG thermograms represented in Figure 4a-c. All thermograms did not show any weight loss below 150 °C to confirm the hydrophobicity of and IPy-IL, AIPy-PIL and AIPy-TIL reduces the moisture uptakes of the prepared ILs although they are fairly good soluble in water. The IPy-IL, AIPy-PIL and AIPy-TIL thermograms show two degradation steps to confirm the initial degradation and final degradation weights loss. The initial degradation step used to determine the initial degradation temperatures (IDTs) of ILs that lost below 5 wt.% of its original weights. The IDTs of IPy-IL, AIPy-PIL and AIPy-TIL are 200, 285 and 300 °C, respectively (Figure 4a-c).

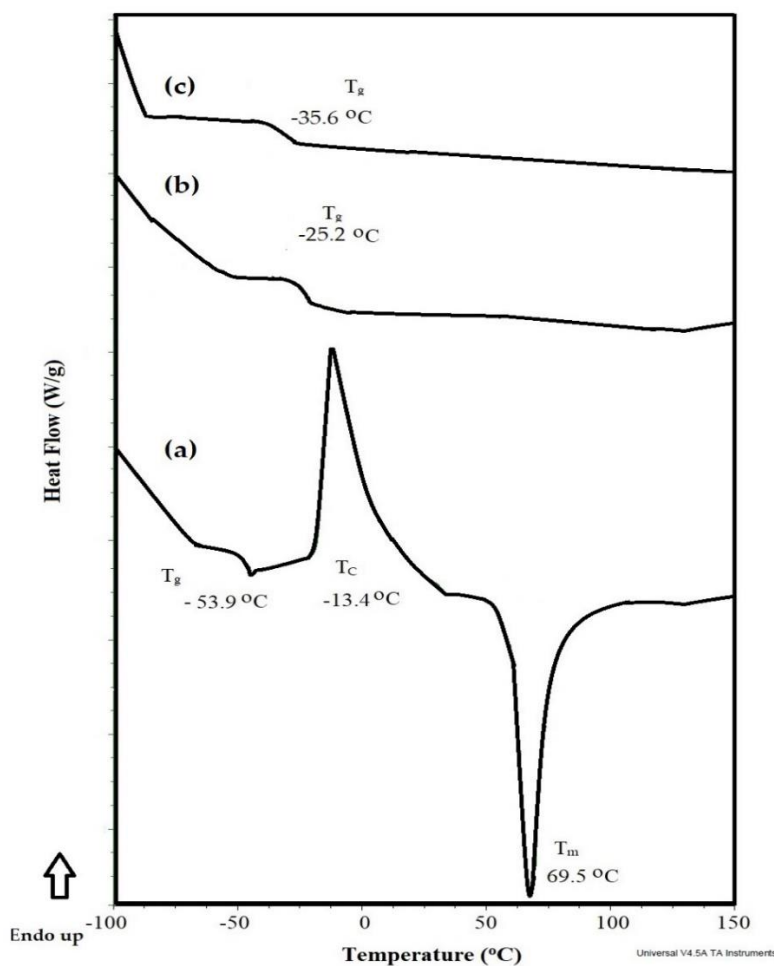


**Figure 3.** DSC thermograms of a) IPy-IL and b) AIPy-IL.

These data prove that the amination of IPy-IL with PEHA or TETA increase its thermal stability due to replacement of hydroxyl group with polyamines [34]. The weight lost (Wt.%) during the first step in case of increases in the order AIPy-PIL > AIPy-TIL > IPy-IL to confirm that the increasing of ILs basicity decreases the initial weight loss percentages due to increasing degradation of nitrogen that increased in case of AIPy-PIL [35]. The second degradation step represents the degradation of IL backbone was used to determine the maximum decomposition temperature ( $T_{max}$ ). The  $T_{max}$  values of IPy-IL, AIPy-PIL and AIPy-TIL are 330, 408 and 420 °C, respectively. The remained residual at 750 °C ( $R_s$  %) confirms the formation of cross-linked cyclic carbon and nitrogen residue obtained from higher thermal stable and lower vapour pressure ionic liquids [36]. The  $R_s$  % of IPy-IL, AIPy-PIL and AIPy-TIL are 5, 8 and 12 wt.% (Figure 5a-c) confirms the lower vapour pressure of AIPy-TIL more than AIPy-PIL pr IPy-IL.

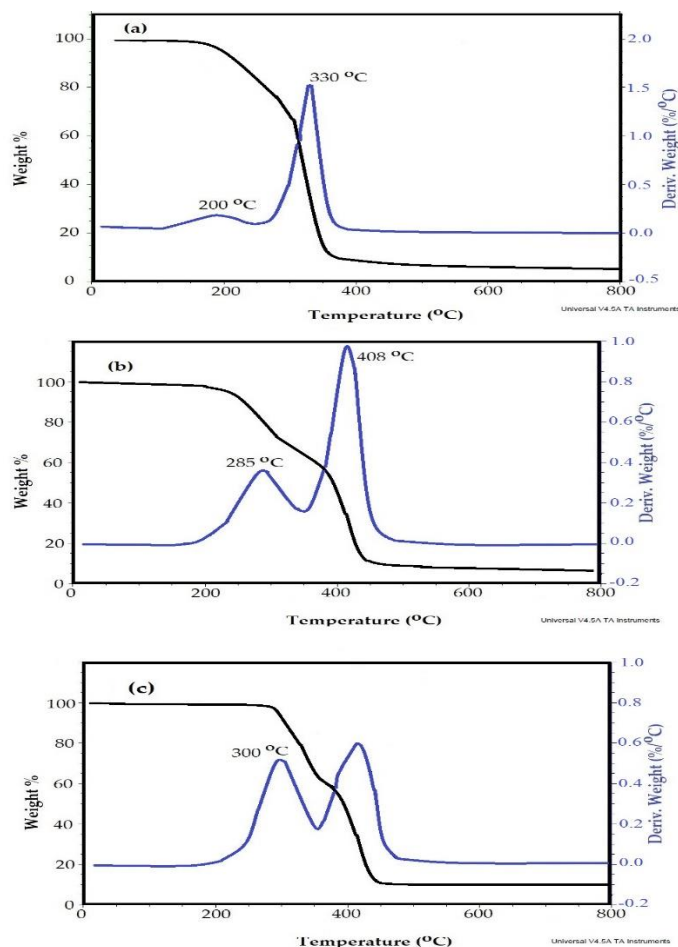


**Figure 4.** TGA-DTG thermograms of a) IPy-IL, b) AIPy-TIL and c) AIPy-PIL.

### 3.2. Curing of epoxy resin with AIPy-TIL and AIPy-PIL

The stoichiometric ratio for part of TETA, PEHA, AIPy-TIL and AIP-PIL per hundred of DGEBA epoxy resin (Phr) can be calculated from the equation:

$$\text{Phr} = [(\text{TAV} \times 100) / (\text{EEW})] \quad (1)$$

Where EEW and TAV are the epoxy equivalent weight and amine values of the hardener that determined experimentally (Table1). The curing agents based on TETA, PEHA, AIPy-TIL or AIP-PIL were mixed separately with DGEBA and heated at constant temperatures ranged from 35 to 55 °C to determine the maximum curing times ( $t_{\text{max}}$ ) and temperatures,  $T_{\text{max}}$ , as reported in the experimental section and represented in both figures 5a-d and Table2. The data (Table 2 and Figure 5a-d) elucidate that the  $t_{\text{max}}$  data were highly affected by changing the curing agent types rather than  $T_{\text{max}}$  that were slightly affected by the changing of the curing agents. Moreover, it was also noticed that the presence of AIPy-TIL and AIP-PIL increasing the curing time  $t_{\text{max}}$  data when were used as curing agent to DGEBA instead PEHA and TEA. These data mean that the presence of imidazolium and pyridinium nitrogen as well as one side of primary amine group reduce the fast curing of DGEBA with the terminal diamino groups of either PEHA or TEA. These data also confirm that the AIPy-TIL and AIP-PIL can also produce

homogeneous cured epoxy networks with controlled crosslinking densities by maintaining the fast curing times [37]. It was previously reported that, the reaction of epoxide groups with primary amines can produces either hydroxyl groups or ether functionalized groups in the epoxy networks through nucleophilic substitution reaction of primary or secondary amine groups of the epoxide groups [38]. The second etherification reactions of the produced hydroxyl groups obtained from epoxide ring opening can be occurred at higher temperatures [38]. The presence of either imidazolium nitrogen tertiary amine and secondary amine of PEHA or TETA can catalyse the homopolymerization of epoxy groups [39]. In this respect, the steric hindrance of AIPy-TIL and AIP-PIL will screen for the catalytic effect of a tertiary or secondary amines potential initiator and for the absence of a Lewis base [40].

**Table 2.** Curing Parameters of DGEb with TETA, PEHA, AIPy-TIL or AIP-PIL at Different Temperatures.

Hardener type	DGEb: hardener	Curing parameters at different temperatures					
		35 °C		45 °C		55 °C	
		t <sub>max</sub> minute	T <sub>max</sub> (°C)	t <sub>max</sub> minute	T <sub>max</sub> (°C)	t <sub>max</sub> minute	T <sub>max</sub> (°C)
TETA	7: 1	75	43	60	54	55	65
PEHA	6: 1	55	46	40	52	30	64
AIPy-PIL	4:1	140	43.5	125	54.5	90	63.1
AIPy-TIL	5: 1	120	46	95	56	85	68

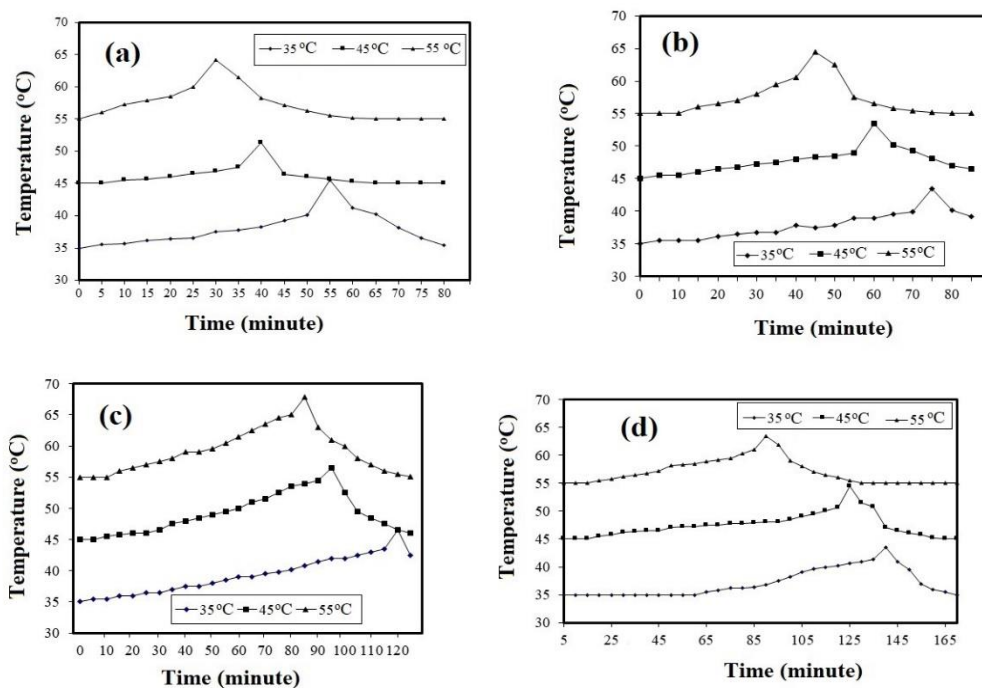
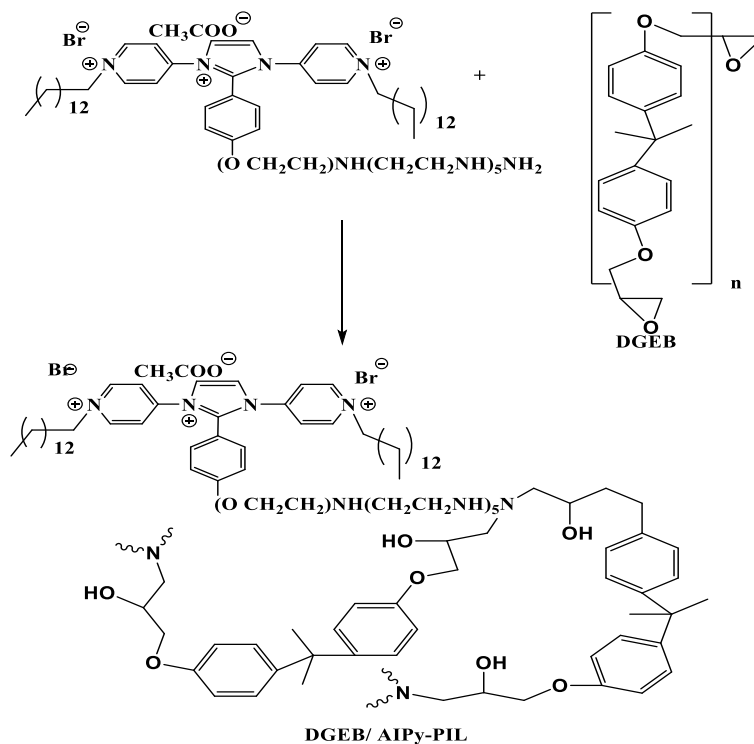


**Figure 5.** Curing exothermic of DGEb with a) PEHA, b) TETA, c) AIPy-TIL and d) AIPy-PIL at different temperatures.



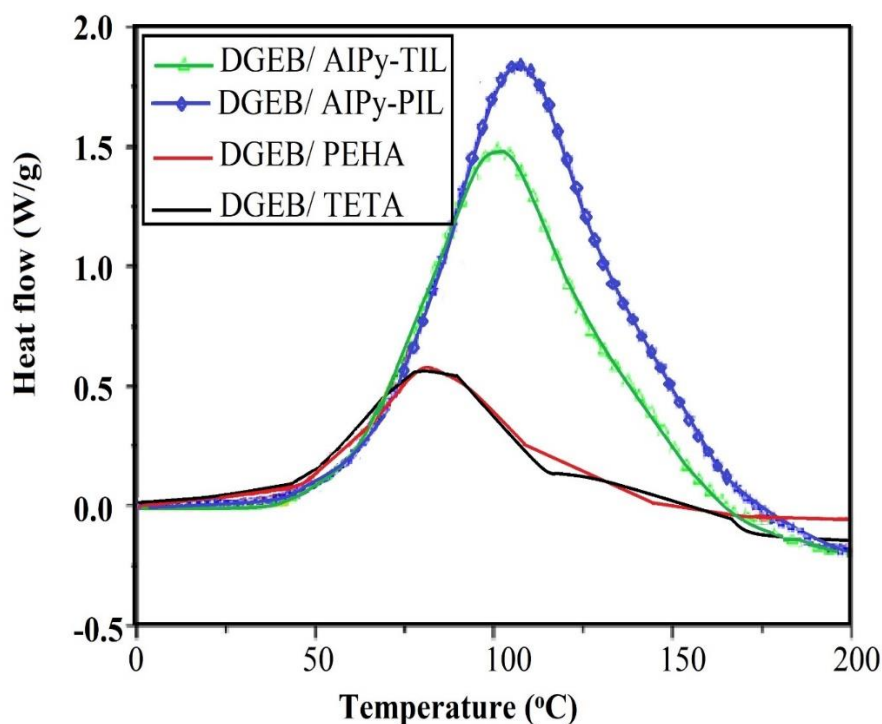
**Scheme 2.** Curing mechanism of DGEb with AIPy-PIL.

The increasing of the curing time  $t_{\max}$  data of the cured epoxy networks in the presence of AIPy-TIL and AIP-PIL confirm that the only proposed mechanism can be illustrated in the scheme 2. Moreover, the carbene mechanism proposed for the imidazolium ILs having the basic counteranion such as (dicyanide, acetate, bromide) was not occurred at lower temperature in this work [40].

The flexibility and rigidity of the cured epoxy networks in the presence of TETA, PEHA, AIPy-TIL or AIP-PIL were estimated from measuring their glass transition temperatures ( $T_g$ ) that evaluated from DSC measurements and represented in Figure 6 and Table 3. The temperatures at the onset ( $T_{\text{onset}}$ ), the termination ( $T_{\text{end}}$ ), and the glass transition exothermic peak ( $T_g$ ) of the reaction, and the reaction heat ( $\Delta H_{\text{total}}$ ) of different systems at heating rates of  $5^\circ\text{C}$  were summarized in Table 3. The  $T_g$  and  $\Delta H_{\text{total}}$  values of the cured DGEb/AIP-PIL system is the highest to elucidate that the formation of ILs increases the curing rate and rigidity of the cured epoxy networks than that cured with either TETA or PEHA. The disappearance of shoulder peaks in DSC curing curves (Figure 6) proves the absence of carbene mechanism of imidazolium ILs [40]. Moreover, the increasing of  $\Delta H_{\text{total}}$  values of the cured DGEb/AIP-PIL and DGEb/AIP-TIL systems more than  $\Delta H_{\text{total}}$  values of the cured DGEb/PEHA or DGEb/TETA systems confirms that both AIP-PIL and AIP-TIL may react completely with DGEb than PEHA or TETA. This was referred to the presence of tertiary amine of IIL can catalyse the curing reactions of DGEb/AIP-PIL and DGEb/AIP-TIL [41].

**Table 3.** Curing exothermic data of the cured DGEb epoxy with different hardener systems.

Epoxy hardener	T <sub>onset</sub> (°C)	T <sub>end</sub> (°C)	T <sub>g</sub> (°C)	ΔH <sub>total</sub> (J/g)
TETA	45.06	118.39	82.96	354.4
PEHA	46.06	121.84	83.34	379.8
AIPy-TIL	48.50	160.40	93.87	460.8
AIPy-PIL	50.30	180.23	98.44	475.3

**Figure 6.** Non-isothermal DSC data of the cured DGEb epoxy with different hardener systems at heating rate 5 °C/min.

### 3.3. Coating, adhesion and salt spray

The curing of the epoxy resin DGEb with polyamine produces hydroxyl groups that linked with metallic substrate especially steel [42]. Moreover, the curing reaction is exothermic and produces heat that form cracks and holes on the coatings surfaces [42]. These holes and cracks diffuse the corrosive environments such as water, salts and dissolved oxygen to start the corrosive of metallic substrates and coatings failure. It is necessary to evaluate the coatings surface morphologies to confirm the disappearance of coatings defects. In this respect, the morphologies of DGEb/TETA, DGEb/PEHA, DGEb/AIPy-TIL and DGEb/AIPy-PIL on the steel surface were evaluated by SEM photos as represented in Figure 7a-d. It was found that the cracks were formed in the fractured DGEb/TETA (Figure 7a) and DGEb/PEHA (Figure 7b). While SEM photos of both DGEb/AIPy-TIL (Figure 7c) and DGEb/AIPy-PIL (Figure 7d) produce uniform surface without cracks or holes. The fractured DGEb/AIPy-PIL film (Figure 7d) shows wrinkling on its surfaces. The disappearance of cracks and holes with appearance of wrinkling confirm the formation of tightly crosslinked epoxy networks with

the presence of dangling chains [43]. The dangling chains are that the chains linked with the epoxy network from one end and the other end does not link with the epoxy networks. These data agree with the curing data that prove both AIP-PIL and AIP-TIL were reacted completely with DGEBA than PEHA or TETA which responsible on the disappearance of cracks and holes.

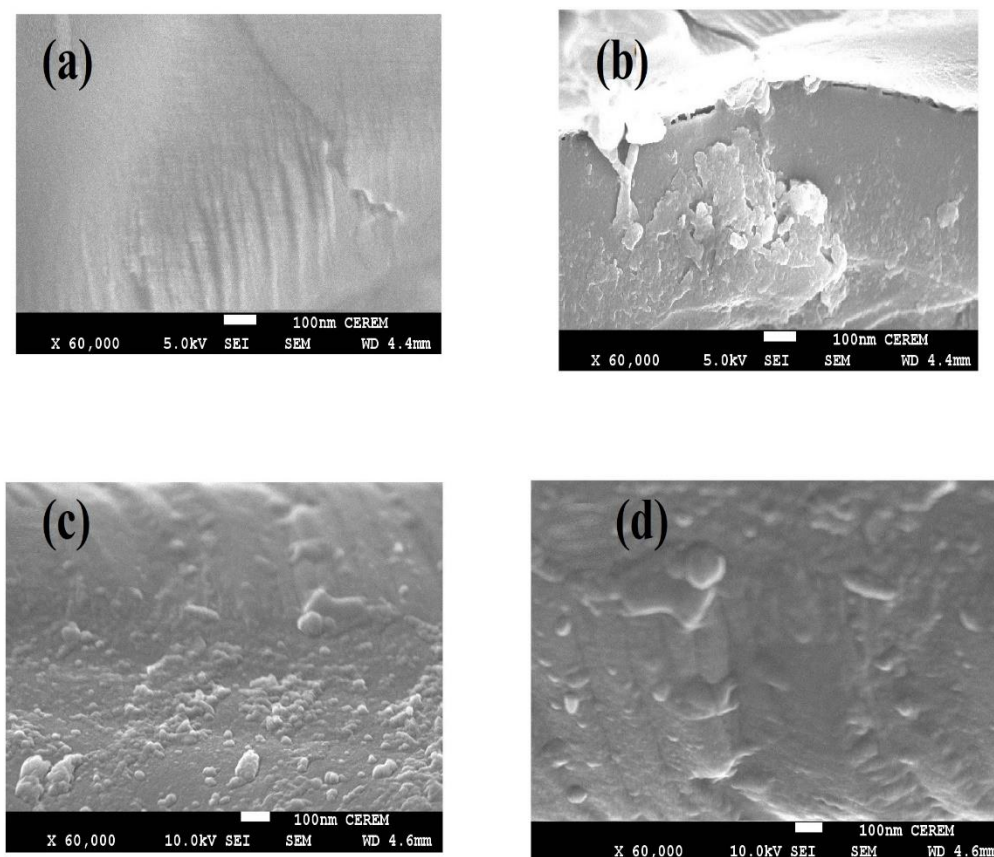


**Figure 7.** SEM photos of fractured a) DGEB/TETA, b) DGEB/PEHA, c) DGEB/ AIPy-TIL and d) DGEB/ AIPy-PIL films.

The adhesion strengths of the cured epoxy resins based on DGEB/TETA, DGEB/PEHA, DGEB/AIPy-TIL and DGEB/ AIPy-PIL on the steel surface were evaluated from pull-off test and summarized in Table 4. The adhesion strength of the coatings is based on the bonding forces among the cured networks, homogeneity of the networks and bonds occurred between the cured networks and substrate [44]. The adhesion strength data of the present system (Table 4) show that the adhesion strengths of DGEB/ AIPy-TIL and DGEB/ AIPy-PIL were improved greater than 15 MPa than their relevant DGEB/TETA and DGEB/PEHA system that have adhesion strengths ranged from 4 to 6 MPa. These data prove that the presence of imidazolium ionic liquids in the hardener chemical structures improved the network curing, homogeneity and produced more hydroxyl groups to increase the bond adhesion between the epoxy networks and steel surface [45, 46]. The increasing of adhesion forces in DGEB/ AIPy-TIL and DGEB/ AIPy-PIL can be also attributed to their hydrophobic chemical structures due to

presence of tetradecyl and phenyl groups that also increase the adhesion and flexibility of the epoxy networks with metallic substrates [47].

The resistances of the cured DGEb/TETA, DGEb/PEHA, DGEb/ AIPy-TIL and DGEb/ AIPy-PIL epoxy systems for salt fogs were evaluated from salt spray resistance test as reported in the experimental section. The results of the salt spray resistance of the cured epoxy systems on the steel surface were summarized in Table 4 and represented in Figure 8a-d. The adhesion test after salt spray test and rusted area on the steel surfaces were evaluated and listed in Table 4. The failure of the salt spray resistance was evaluated from the failure of adhesion strength due to the formation of rust under coatings with increasing the diffusion of salts and humidity in the presence of seawater salt fog. The salt spray resistance data (Table 4) show that the duration time of the cured DGEb/TETA, DGEb/PEHA, DGEb/ AIPy-TIL and DGEb/ AIPy-PIL are 650, 750, 1750 and 2000 h, respectively. These data agree with the increasing of coatings adhesion strengths, homogeneity of the cured epoxy networks (SEM photos, Figure 7a-d) and curing data (DSC data; Figure 6) of DGEb/ AIPy-TIL and DGEb/ AIPy-PIL.

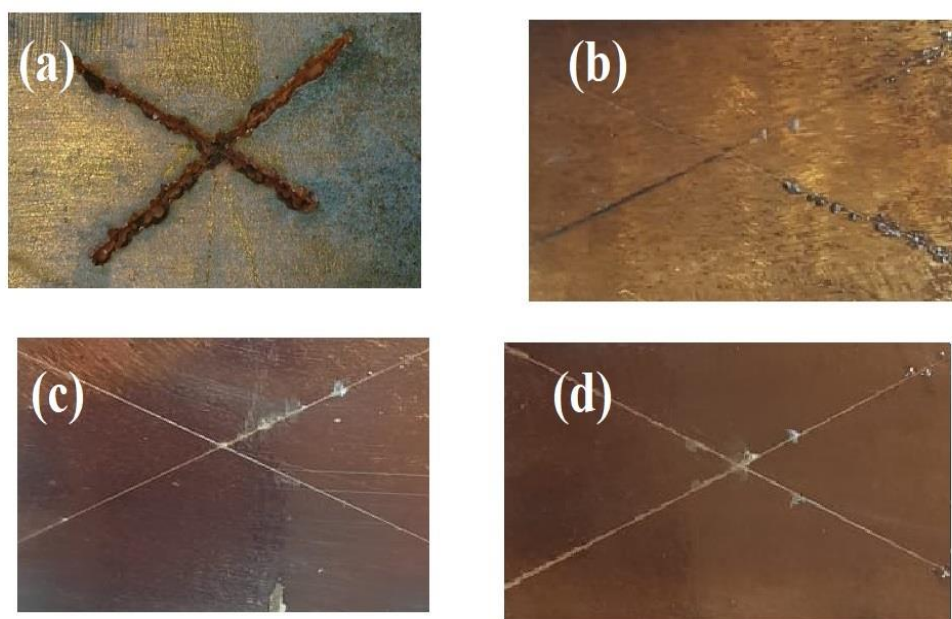


**Figure 7.** Salt spray resistance photos of a) DGEb/TETA, b) DGEb/PEHA, c) DGEb/ AIPy-TIL and d) DGEb/ AIPy-PIL coating films after exposure to salt fog at different exposure times.

It was previously correlated the correlation between salt spray resistance of the organic coatings and their rapid electrochemical measurements to conclude that there the salt fog time-to-failure is depended on the corrosion resistance of coatings as measured by rapid electrochemical data [49, 50]. It can be also suggested that the corrosion of steel in the environments proceeded by anodic iron dissolution and oxygen reductions reactions were based on the diffusion process of oxygen through the solution film was not completely rate-determining in case of salt spray resistance [50]. Moreover, it can be also confirmed that the stronger ability of the organic coatings to resist the diffusion of corrosive oxygen, water humidity and electrolyte from the organic coatings to steel surfaces was not only depended on

their thickness but also based on the strong surface adhesion and crosslinking density of the produced organic epoxy coatings films.

**Table 4.** Salt spray resistance of cured epoxy systems and their adhesion strengths at 37 °C in seawater fogs humidity >98 %.

Sample no.	Exposure time (h)	Disbonded area		ASTM D1654-92 rating	Adhesion strengths (MPa)	
		cm <sup>2</sup>	%		Before salt spray	After salt spray exposure time
DGEB/TETA	650	18.3	15.8	5	5.3	2.5
DGEB/PEHA	750	7.1	6	7	6.8	3.4
DGEB/ AIPy-TIL	1750	13	11	6	15.6	6.3
DGEB/ AIPy-PIL	2000	1.2	1	9	20.6	10.8

Consequently, it can be concluding that the presence of hydrophobic tetradecyl and phenyl groups in the cured DGEB/ AIPy-TIL and DGEB/ AIPy-PIL networks will reduce the diffusion of seawater humidity from the cured films to steel surfaces. Moreover, the presence of imidazolium, pyridinium cations as well as bromide and acetate anions in the chemical structures of the cured DGEB/ AIPy-TIL and DGEB/ AIPy-PIL networks will retard the seawater salt diffusion from the cured films to steel surface. This can be attributed to excellent resistivity of imidazolium and pyridinium ILs to aggregation in seawater salts which improve the DGEB/ AIPy-TIL and DGEB/ AIPy-PIL networks salt diffusion inside coatings to form rust and pitting corrosion.

#### 4. CONCLUSIONS

New amphiphilic ionic liquids combined both imidazolium and pyridinium IL and has hydrophobic and hydrophilic polyamine were prepared. The thermal stability data prove that the amination of IPy-IL with PEHA or TETA increase its thermal stability due to replacement of hydroxyl group with polyamines and the maximum decomposition temperature ( $T_{max}$ ) values of IPy-IL, AIPy-PIL and AIPy-TIL are 330, 408 and 420 °C, respectively. The DSC data confirm that the increasing  $T_g$  values of AIPy-PIL and AIPy-TIL as appeared at -25.2 and -35.6 °C, respectively than IPy-IL confirms that the amination with PEHA and TETA leads to increase its rigidity and they behave as ILs to melt below 100 °C. The curing of epoxy resin with the prepared ILs confirm that the presence of AIPy-TIL and AIP-PIL increases the curing time  $t_{max}$  data when were used as curing agent to DGEB instead PEHA and TEA. The  $T_g$  data of the cured DGEB/ PEHA or DGEB/ TETA systems confirm that both AIP-PIL and AIP-TIL may react completely with DGEB than PEHA or TETA which responsible on the disappearance of cracks and holes and formation of wrinkled morphologies with formation of homogeneous networks. The presence of tetradecyl and phenyl groups in the chemical structures of AIPy-PIL and AIPy-TIL

increase the adhesion and flexibility of the epoxy networks with metallic substrates. The presence of imidazolium, pyridinium cations as well as bromide and acetate anions in the chemical structures of the cured DGEb/ AIPy-TIL and DGEb/ AIPy-PIL networks will retard the seawater salt diffusion from the cured films to steel surface to resist the diffusion of seawater salt fog more than 2000 h. It was also attributed to excellent resistivity of imidazolium and pyridinium ILs to aggregation in seawater salts which improve the DGEb/ AIPy-TIL and DGEb/ AIPy-PIL networks salt diffusion inside coatings to form rust and pitting corrosion.

#### ACKNOWLEDGEMENT

This research has been funded by scientific research deanship at university of Hail- Saudi Arabia through project number RG-191200.

#### References

1. P. A. Sørensen, S. Kiil, K. Dam-Johansen and C. E. Weinell, *J. Coat. Tech. Res.*, 6 (2009) 135.
2. J. Kellner, A. Doheny and B. Patil, *Mater. Perform.*, 37 (1998) 28.
3. K. Tamalmani and H. Husin, *Appl. Sci.*, 10 (2020) 3389.
4. M. Morell, A. Lederer, X. Ramis, B. Voit and A. Serra, *J. Polym. Sci., Part A: Polym. Chem.*, 49 (2011) 2395.
5. I.-C. Mirică, G. Furtos, B. Bâldea, O. Lucaciu, A. Ilea, M. Moldovan and R.-S. Câmpian, *Materials*, 13 (2020) 1477.
6. A. Radhamani, H. C. Lau and S. Ramakrishna, *J. Coat. Mat.*, 54 (2020) 681.
7. Z. T. Khodair, A. A. Khadom and H. A. Jasim, *J. Mat. Res. Tech.*, 8 (2019) 424.
8. G. Mittal, V. Dhand, K. Y. Rhee, S.-J. Park and W. R. Lee, *J. Ind. Eng. Chem.*, 21 (2015) 11.
9. P.-N. Wang, T.-H. Hsieh, C.-L. Chiang and M.-Y. Shen, *J. Nanomat.*, 2015 (2015) 838032.
10. F. C. Binks, G. Cavalli, M. Henningsen, B. J. Howlin and I. Hamerton, *React. Funct. Polym.*, 133 (2018) 9.
11. F. C. Binks, G. Cavalli, M. Henningsen, B. J. Howlin and I. Hamerton, *Thermochim. Acta*, 663 (2018) 19.
12. Y. Q. Shi, T. Fu, Y.-J. Xu, D.-F. Li, X.-L. Wang and Y.-Z. Wang, *Chem. Eng. J.*, 354 (2018) 208.
13. A. A. Silva, S. Livi, D. B. Netto, B. G. Soares, J. Duchet and J.-F. Gérard, *Polymers*, 54 (2013) 2123.
14. M. A. M. Rahmathullah, A. Jeyarajasingam, B. Merritt, M. VanLandingham, S. H. McKnight and G. R. Palmese, *Macromolecules*, 42 (2009) 3219.
15. K. Kowalczyk and T. Szychaj, *Polimery*, 48 (2003) 833.
16. M. A. M. Rahmathullah, A. Jeyarajasingam, B. Merritt, M. VanLandingham, S. H. McKnight and G. R. Palmese, *Macromolecules*, 42 (2009) 3219.
17. H. Maka, T. Szychaj and R. Pilawka, *Ind. Eng. Chem. Res.*, 51 (2012) 5197.
18. F. C. Binks, G. Cavalli, M. Henningsen, B. J. Howlin and I. Hamerton, *Polymers*, 139 (2018) 163.
19. S. Livi, L. C. Lins, L. B. Capeletti, C. Chardin, N. Halawani, J. Baudoux and M. B. Cardoso, *Eur. Polym. J.*, 116 (2019) 56.
20. Y.-J. Xu, X.-H. Shi, J.-H. Lu, M. Qi, D.-M. Guo, L. Chen and Y.-Z. Wang, *Comp. Eng.*, 184 (2020) 107673.
21. B. G. Soares, S. C. Ferreira and S. Livi, *Appl. Clay Sci.*, 135 (2017) 347-354.
22. L. F. C. Souto and B. G. Soares, *Prog. Org. Coat.*, 143 (2020) 105598.
23. A. O. Ezzat, A. M. Atta, H. A. Al-Lohedan and A. Aldalbahi, *J. Mol. Liq.*, 312 (2020) 113407.

24. M. H. Wahby, A. M. Atta, Y. M. Moustafa, A. O. Ezzat and A. I. Hashem, *Coatings*, 10 (2020) 1201.
25. ASTM B117-03, Standard Practice for Operating Salt Spray (Fog) Apparatus, ASTM International, West Conshohocken, PA (2003). [www.astm.org](http://www.astm.org)
26. ASTM D610-95, Standard Test Method for Evaluating Degree of Rusting on Painted Steel Surfaces, ASTM International, West Conshohocken, PA, (2001). [www.astm.org](http://www.astm.org).
27. ASTM D3359-17, Standard Test Methods for Rating Adhesion by Tape Test, ASTM International, West Conshohocken, PA (2017). [www.astm.org](http://www.astm.org).
28. V. Malshe and N. S. Sangaj, *Prog. Org. Coat.*, 53 (2005) 207.
29. STM D522-93a, Standard Test Methods for Mandrel Bend Test of Attached Organic Coatings, ASTM International, West Conshohocken, PA (2001). [www.astm.org](http://www.astm.org).
30. H. Taghiyari, A. Esmailpour and A. Papadopoulos, *Coatings*, 9 (2019) 723.
31. J. W. Choi, F. Medina, C. Kim, D. Espalin, D. Rodriguez, B. Stucker and R. Wicker, *J. Mater. Process. Technol.*, 211 (2011) 424.
32. G.-h. Tao, L. He, N. Sun and Y. Kou, *Chem. Commun.*, (2005) 3562.
33. F. U. Shah, S. Glavatskih, P. M. Dean, D. R. MacFarlane, M. Forsyth and O. N. Antzutkin, *J. Mat. Chem.*, 22 (2012) 6928.
34. A. S. More, A. S. Patil and P. P. Wadgaonkar, *Polym. Deg. Stab.*, 95 (2010) 837.
35. Y. Cao and T. Mu, *Ind. Eng. Chem. Res.*, 53 (2014) 8651.
36. S. Cheng, B. Chen, L. Qin, Y. Zhang, G. Gao and M. He, *RSC Adv.*, 9 (2019) 8137.
37. S. b. Livi, C. Chardin, L. C. Lins, N. Halawani, S. b. Pruvost, J. Duchet-Rumeau, J.-F. O. Gérard and J. r. m. Baudoux, *ACS Sust. Chem. Eng.*, 7 (2019) 3602.
38. S. Zheng, J. Pascault and R. Williams, *Pascault, JP, Williams, RJJ, Eds*, 2010.
39. M. Heise and G. Martin, *Macromolecules*, 22 (1989) 99.
40. H. Maka, T. Spsychaj and R. Pilawka, *Ind. Eng. Chem. Res.*, 51 (2012) 5197.
41. J. Wan, C. Li, Z.-Y. Bu, C. J. Xu, B.-G. Li and H. Fan, *Chem. Eng. J.*, 188 (2012) 160.
42. M. H. Wahby, A. M. Atta, Y. M. Moustafa, A. O. Ezzat and A. I. Hashem, *Coatings*, 11 (2021) 83.
43. Y. Wang and J. Xiao, *Soft Mat.*, 13 (2017) 5317.
44. H. Wei, J. Xia, W. Zhou, L. Zhou, G. Hussain, Q. Li and K. K. Ostrikov, *Comp. Eng.*, 193 (2020) 108035.
45. Z. Jiang, Q. Wang, L. Liu, Y. Zhang, F. Du and A. Pang, *Ind. Eng. Chem. Res.*, 59 (2020) 3024.
46. A. Dzienia, M. Tarnacka, K. Koperwas, P. Maksym, A. Zięba, J. Feder-Kubis, K. Kamiński and M. Paluch, *Macromolecules*, 53 (2020) 6341.
47. K. Huang, Y. Zhang, M. Li, J. Lian, X. Yang and J. Xia, *Prog. Org. Coat.*, 74(2012) 240.
48. P. Verge, V. Toniazzo, D. Ruch and J. A. Bomfim, *Ind. Crop. Prod.*, 55 (2014) 180.
49. M. Kendig , S. Jeanjaquet, R. Brown and F. Thomas, *Corrosion*, Houston Tx.; 54 (1998) 61.
50. M. Ito, A. Ooi, E. Tada and A. Nishikata, *J. Electrochem. Soc.*, 167 (2020) 101508.